

Mechanistic Analysis of Rigid Pavement for Wheel Load Stresses by Finite Element Method Considering Different Sub-Grade

¹Mohd. Imran khan, (Assistant professor) Dr. Ahmad ali khan,²(HOD) Dr. Shalini yadav³(HOD)

¹Civil Engineering Department, Technocrat Institute of Technology, Bhopal, Pin Code, 462022, Madhya Pradesh, India

²Civil Engineering Department, All saints College of Engineering, Bhopal, Pin code 462036, Madhya Pradesh, India

³Civil Engineering Department, aisect university, Bhopal Pin code 464993, Madhya Pradesh, India

Abstract

In this research work it was aimed to generate charts for flexural stresses due to wheel loads using finite element method. ANSYS software is basically software for finite element technique. For generating the charts, edge loading condition was considered which critical case for wheel load stresses is. The pavement slab has been analysed for different axle loads and subgrade using finite element method, and results are compared with Westergaard's analysis. Also it was aimed to compare the results with those given by Westergaard's solution and IRC 58 – 2002 design charts.

Keywords: Concrete slab, Winkler foundation, Stresses Analysis, rigid pavement, finite element analysis etc.

I. INTRODUCTION

In recent years, cement concrete pavements are being adopted in many new road projects in India in view of their longer services lives, lesser maintenance requirements and smoother riding surface. The current practice of constructing concrete pavement on Indian highways is to provide a granular sub-base over the sub-grade to be followed by a Dry lean concrete base with the concrete slab on top which is called rigid pavement.

Rigid pavements are those which possess flexural strength & flexural rigidity. The stresses are not transferred from grain to grain to the lower layer as in the case of flexible pavement layers. The rigid pavement are made of Portland cement concrete either plain, reinforced or prestressed concrete. The plain cement concrete slabs are expected to take up about 40kg/cm² flexural stress. Tensile stress are developed due to the bending of the slab under wheel loads & temperature variation. The rigid pavement consists of three components a)soil sub-grade b)base course c)cement concrete slab as shown in figure 1.1.

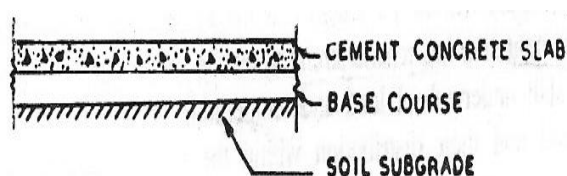


Fig. 1.1: Rigid pavement

1.1 Types of Rigid Pavement

Rigid pavements are differentiated into three major categories by their means of crack control.

- **Jointed Plain Concrete Pavement (JPCP):**

This is the most common type of rigid pavement. JPCP controls cracks by dividing the pavement into individual slabs separated by contraction joint slabs are typically one lane wide and between 3.7 m and 6.1 m long. JPCP does not use any reinforcing steel but does use dowel bars and tie bars.

- **Jointed Reinforced Concrete Pavements (JRCP):**

As with JPCP, JRCP controls cracks by dividing the pavement into individual slabs separated by contraction joints. However these slabs are much longer (as long as 15 m) than JPCP slabs, so JRCP uses reinforcing steel with each slab to control with in slab cracking. This pavement type is no longer constructed due to some long term performance problems.

- **Continuously Reinforced Concrete Pavements (CRCP)**

This type of rigid pavement uses reinforcing steel rather than contraction joints for crack control. Transverse cracks are allowed to form but are held tightly together with continuously reinforcing steel. Research has shown that the maximum allowable design crack width is about 0.5mm.

II. LITERATURE REVIEW

In the early days of highway engineering, rigid-pavement slabs were constructed directly upon the subgrade without giving consideration to subgrade type and drainage conditions. Slabs as little as 150mm uniform thickness were commonly built. With increasing truck traffic, particularly just before the second world war, it became evident that subgrade type played an important role in the performance of the pavements. In fact, pavement pumping was described as early as 1932.

In the period between 1930 and 1940, it was not uncommon to build thickened-edge sections, for example, 8-6, which indicates center thicknesses of 6 inches and the edge thickened to 8 inches. Thickened-edge sections were constructed to offer increased resistance to high stress conditions at the edges of the pavements. At about that time, pavements 6264mm wide were not uncommon, with the result that heavy trucks traveled very close to the pavement edge.

After pavement pumping became critical on some of the major highways, particularly in the eastern states, rigid highway slabs were constructed on granular base courses of varying thickness to protect against loss of subgrade support due to pumping. Many studies were made of the factors which affect pumping action, and criteria were evolved for design of base courses for correction of the action. Pavement thicknesses gradually increased until 250mm uniform thicknesses became common.

Just after the second world war, many states sanctioned the construction of toll roads to meet heavy demands placed upon them for additional expressways. Use of rigid slabs 250mm thick became widespread on most turnpikes. As an example of the evolution of rigid-pavement design, the original Turnpike was constructed using 230mm uniform flat slabs built directly upon subgrade. This resulted in severe pumping distress after a period of about 10 years. As a consequence, later extensions to this turnpike were constructed on 150mm of prepared open-graded base course and the slab thickness was increased to a uniform 250mm.

Chih-Ping et al[2]. Studied dynamic responses of concrete pavement subjected to moving loads by using the three-dimensional (3D) finite-element method in conjunction with Newmark integration scheme. The dynamic vehicle-pavement-foundation interaction effects are considered in the 3D finite-element algorithm. The moving vehicle loads are modeled as lumped masses each supported by a spring-dashpot suspension system and having a specified

horizontal velocity and acceleration. Concrete pavements are considered to respond elastically and are represented by a series of brick elements. The present formulation considers a linear viscoelastic foundation model (Kelvin model) consisting of a system of discrete linear springs and dashpots. The interaction between concrete pavements and underlying soil foundation was considered.

Shunanfa Chen et al [7]. have done the finite element stress analysis of concrete pavement with subbase voids, Cracks at the corners and along the edges of concrete slabs appear frequently on Portland cement concrete pavements. This study analyzes the relationship between the loss of support underneath pavement slabs and the premature failures of pavement slabs. The combined effects of the size of subbase void and the magnitude of vehicle loading on pavement stress were examined through three-dimensional finite element analysis. This paper presented the values of flexural tensile stresses at the corner and along the longitudinal and transverse joint edges of concrete slabs under different loadings and the changing patterns of the stresses with various sizes of subbase voids.

K.Bhattacharya[3]. has reported studies on edge stresses of plain concrete pavements, Edge stresses of plain concrete slabs-on-grade were computed by finite element methods using 3-dimensional (3D) brick element and spring elements for slab and soil, respectively. Analysis was carried out for a wide range of load and slab-soil combinations, with an aim to derive a unified expression on edge stresses. The soil as 'Winkler type' represented by elastic springs and their stiffness was derived from modulus of sub-grade reaction. The influence of any particular base or sub-base on edge stresses was not studied here. The expression was validated with both experimental and theoretical results obtained from literature.

S.Santosh Kumar et al[8]. have studied on mechanistic design of concrete pavement, They described examples of thickness design of various types of concrete pavements considering the combined action of axle loads of commercial vehicles and non-linear temperature distribution. Finite element method was adopted for the analysis's of stresses. The possibility of top-down cracking due to axle loads during the night hours has also been examined. It is found that the slabs may undergo top-down cracking when the front and rear axles lie within the transverse joints of slab. They concluded that less thickness of slab is required if there is a tied concrete shoulder or when

the slab has a widened outer lane. Thickness of the pavement slab can be reduced substantially if it is bonded to the cemented subbase. Higher modulus of subgrade reaction causes higher flexural stresses due to combined action of axle load and warping during the day time as compared to those subgrades with lower modulus of subgrade reaction.

Finite Element Modelling

In the present study, a 3-dimensional finite element model for concrete pavement system has been developed. For this, the structural analysis package ‘ANSYS’ (Version 10.0)[1].has been used. 3-D brick element SOLID45, having 8 nodes with three degrees of freedom per node translations in the nodal x, y and z directions, are used to model the concrete slab as well as the base. The sub-grade is modelled as Winkler foundation that consists of a bed of closely spaced, independent, linear springs. Each spring deforms in response to the vertical load applied directly to that spring, and is independent of any shear force transmitted from adjacent areas in the foundation. Spring elements namely COMBIN 14 are used to represent the Winkler foundation which has three degrees of freedom at each node- translations in the nodal x, y, and z directions. The effective normal stiffness of the element is obtained by multiplying the modulus of sub-grade reaction with the influencing area of that element.

III. DETAILS OF THE RIGID PAVEMENT MODEL

Data used

The concrete slabs are 4.5m x 3.7m (Fig 4.1) in dimension having different thickness the concrete properties are

- Modulus of elasticity, $E = 3 \times 10^{10} \text{ N/m}^2$
- Poisson's ratio, $\mu = 0.15$
- Co-efficient of thermal expansion, $\alpha = 10 \times 10^{-6} / ^\circ\text{C}$
- Density, $\gamma = 24000 \text{ N/m}^3$

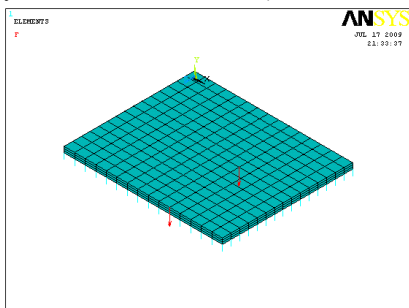


Fig 4.1: Model – Slab pavement with Winkler foundation with a 60KN axle load at the edge of the slab

IV. SAMPLE REPRESENTATION OF WESTERGAARD METHOD STRESSES Comparison of ANSYS results with Westergaard's (Single axle load = 60 KN)

Table 5.1: For slab thickness 160mm

Sl. No.	Stress in N/mm ² by analysis results	Stress in N/mm ² by Westergaard's	Axle load in KN	K in N/mm ³
1.	2.22	2.67	60	0.06
2.	2.18	2.58	60	0.08

Table 5.2: For slab thickness 180mm

Sl. No.	Stress in N/mm ² by analysis results	Stress in N/mm ² by Westergaard's	Axle load in KN	K in N/mm ³
1.	2.13	2.08	60	0.06
2.	2.1	2.02	60	0.08

Table 5.3: For slab thickness 200mm

Sl. No.	Stress in N/mm ² by analysis results	Stress in N/mm ² by Westergaard's	Axle load in KN	K in N/mm ³
1.	1.93	1.75	60	0.06
2.	1.92	1.7	60	0.08

Table 5.4: For slab thickness 220mm

Sl. No.	Stress in N/mm ² by analysis results	Stress in N/mm ² by Westergaard's	Axle load in KN	K in N/mm ³
1.	1.75	1.49	60	0.06
2.	1.74	1.44	60	0.08

Table 5.5: For slab thickness 240mm

Sl. No.	Stress in N/mm ² by analysis results	Stress in N/mm ² by Westergaard's	Axle load in KN	K in N/mm ³
1.	1.51	1.23	60	0.06
2.	1.5	1.19	60	0.08

Table 5.6: For slab thickness 260mm

Sl. No.	Stress in N/mm ² by analysis results	Stress in N/mm ² by Westergaard's	Axle load in KN	K in N/mm ³
1.	1.29	1.07	60	0.06
2.	1.28	1.04	60	0.08

Table 5.7: For slab thickness 280mm

Sl. No.	Stress in N/mm ² by analysis results	Stress in N/mm ² by Westergaard's	Axle load in KN	K in N/mm ³
1.	1.08	0.911	60	0.06
2.	1.08	0.884	60	0.08

Table 5.8: For slab thickness 300mm

Sl. No.	Stress in N/mm ² by analysis results	Stress in N/mm ² by Westergaard's	Axle load in KN	K in N/m ³
1.	0.911	0.81	60	0.06
2.	0.9	0.787	60	0.08

Table 5.9: For slab thickness 320mm

Sl. No.	Stress in N/mm ² by analysis results	Stress in N/mm ² by Westergaard's	Axle load in KN	K in N/m ³
1.	0.889	0.702	60	0.06
2.	0.881	0.681	60	0.08

Table 5.10: For slab thickness 340mm

Sl. No.	Stress in N/mm ² by analysis results	Stress in N/mm ² by Westergaard's	Axle load in KN	K in N/m ³
1.	0.745	0.633	60	0.06
2.	0.736	0.614	60	0.08

Table 5.11: For slab thickness 360mm

Sl. No.	Stress in N/mm ² by analysis results	Stress in N/mm ² by Westergaard's	Axle load in KN	K in N/m ³
1.	0.736	0.556	60	0.06
2.	0.728	0.539	60	0.08

V. FLEXURAL STRESSES DUE TO EDGE LOADING CONDITION (SINGLE AXLE LOAD 60KN)

Table A1.1: The maximum flexural tensile stresses and deflection for slab thickness 160mm

Sl. No.	Stress in N/mm ²	Deflection in mm	Axle load in KN	K in N/mm ³
1.	2.22	0.520	60	0.06
2.	2.18	0.381	60	0.08
3.	2.16	0.282	60	0.10
4.	2.12	0.187	60	0.15
5.	2.09	0.0753	60	0.30

Table A1.2: The maximum flexural tensile stresses and deflection for slab thickness 180mm

Sl. No.	Stress in N/mm ²	Deflection in mm	Axle load in KN	K in N/mm ³
1.	2.13	0.309	60	0.06
2.	2.10	0.297	60	0.08
3.	2.09	0.233	60	0.10
4.	2.07	0.135	60	0.15
5.	2.05	0.0455	60	0.30

Table A1.3: The maximum flexural tensile stresses and deflection for slab thickness 200mm

Sl. No.	Stress in N/mm ²	Deflection in mm	Axle load in KN	K in N/mm ³
1.	1.93	1.238	60	0.06
2.	1.92	0.929	60	0.08
3.	1.90	0.548	60	0.10
4.	1.89	0.250	60	0.15
5.	1.87	0.0823	60	0.30

Table A1.4: The maximum flexural tensile stresses and deflection for slab thickness 220mm

Sl. No.	Stress in N/mm ²	Deflection in mm	Axle load in KN	K in N/mm ³
1.	1.75	0.297	60	0.06
2.	1.74	0.217	60	0.08
3.	1.73	0.178	60	0.10
4.	1.72	0.0895	60	0.15
5.	1.71	0.0574	60	0.30

Table A1.9: The maximum flexural tensile stresses and deflection for slab thickness 320mm

Sl. No.	Stress in N/mm ²	Deflection in mm	Axle load in KN	K in N/mm ³
1.	0.889	1.593	60	0.06
2.	0.881	1.289	60	0.08
3.	0.875	0.532	60	0.10
4.	0.868	0.291	60	0.15
5.	0.859	0.730	60	0.30

Table A1.5: The maximum flexural tensile stresses and deflection for slab thickness 240mm

Sl. No.	Stress in N/mm ²	Deflection in mm	Axle load in KN	K in N/mm ³
1.	1.51	0.827	60	0.06
2.	1.50	0.937	60	0.08
3.	1.49	0.108	60	0.10
4.	1.48	0.419	60	0.15
5.	1.47	0.381	60	0.30

Table A1.10: The maximum flexural tensile stresses and deflection for slab thickness 340mm

Sl. No.	Stress in N/mm ²	Deflection in mm	Axle load in KN	K in N/mm ³
1.	0.745	0.0867	60	0.06
2.	0.736	0.0637	60	0.08
3.	0.730	0.0549	60	0.10
4.	0.720	0.0445	60	0.15
5.	0.712	0.0308	60	0.30

Table A1.6: The maximum flexural tensile stresses and deflection for slab thickness 260mm

Sl. No.	Stress in N/mm ²	Deflection in mm	Axle load in KN	K in N/mm ³
1.	1.29	0.0948	60	0.06
2.	1.28	0.0723	60	0.08
3.	1.27	0.0626	60	0.10
4.	1.26	0.0504	60	0.15
5.	1.25	0.0373	60	0.30

Table A1.11: The maximum flexural tensile stresses and deflection for slab thickness 360mm

Sl. No.	Stress in N/mm ²	Deflection in mm	Axle load in KN	K in N/mm ³
1.	0.736	0.172	60	0.06
2.	0.728	0.165	60	0.08
3.	0.723	0.150	60	0.10
4.	0.715	0.140	60	0.15
5.	0.707	0.0408	60	0.30

Table A1.7: The maximum flexural tensile stresses and deflection for slab thickness 280mm

Sl. No.	Stress in N/mm ²	Deflection in mm	Axle load in KN	K in N/mm ³
1.	1.09	0.0759	60	0.06
2.	1.08	0.0643	60	0.08
3.	1.07	0.0568	60	0.10
4.	1.06	0.0461	60	0.15
5.	1.05	0.0330	60	0.30

Table A1.8: The maximum flexural tensile stresses and deflection for slab thickness 300mm

Sl. No.	Stress in N/mm ²	Deflection in mm	Axle load in KN	K in N/mm ³
1.	0.911	0.885	60	0.06
2.	0.90	0.684	60	0.08
3.	0.893	0.671	60	0.10
4.	0.882	0.307	60	0.15
5.	0.870	0.108	60	0.30

COMPARISON BETWEEN IRC 58-2002 AND ANSYS

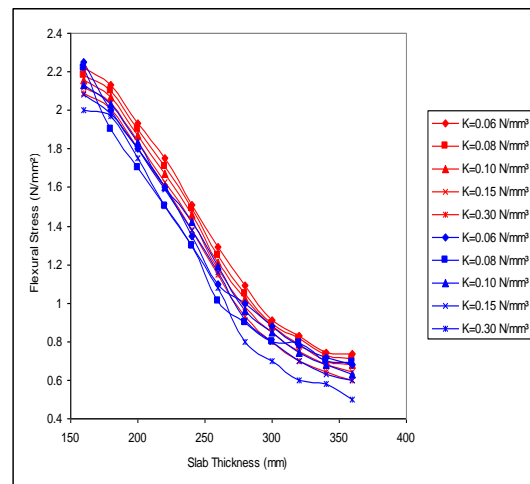


Fig. 5.1: Stresses in Rigid Pavement (Single axle load = 60kN)

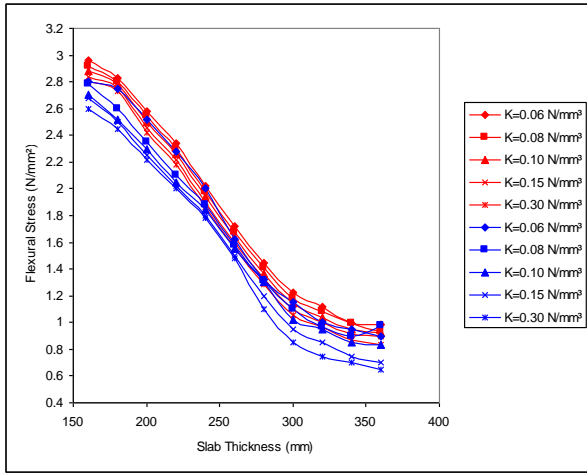


Fig. 5.2: Stresses in Rigid Pavement (Single axle load = 80kN)

STRESS CHART FOR CONCRETE PAVEMENT

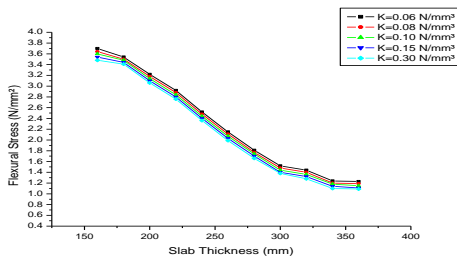


Fig. 5.3: Stresses in rigid pavement (single axle load = 100kN)

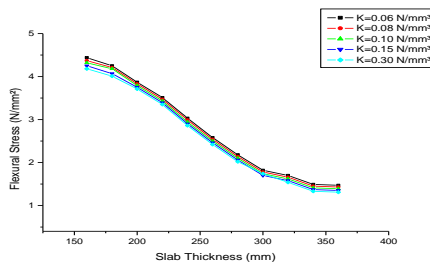


Fig. 5.4: Stresses in rigid pavement (single axle load = 120kN)

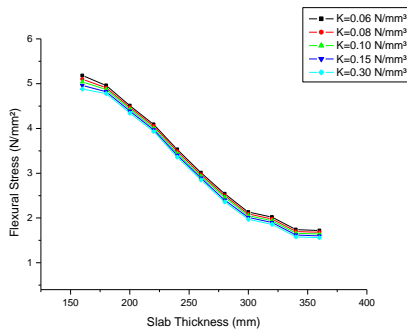


Fig. 5.5: Stresses in rigid pavement (single axle load =140kN)

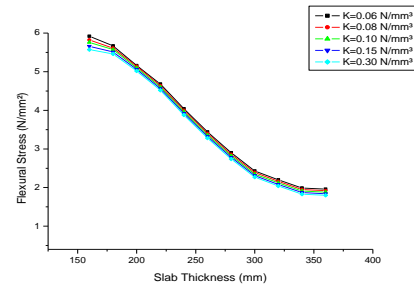


Fig. 5.6: Stresses in rigid pavement (single axle load = 160kN)

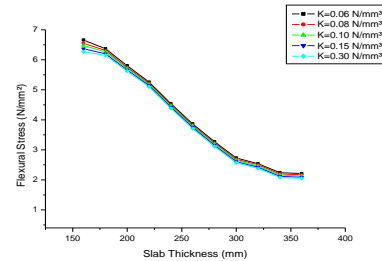


Fig. 5.7: Stresses in rigid pavement (single axle load = 180kN)

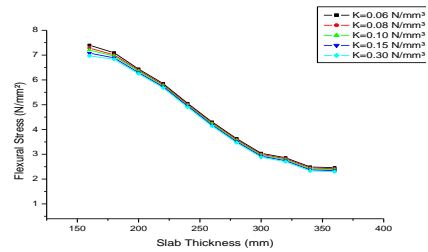


Fig. 5.8: Stresses in rigid pavement (single axle load = 200kN)

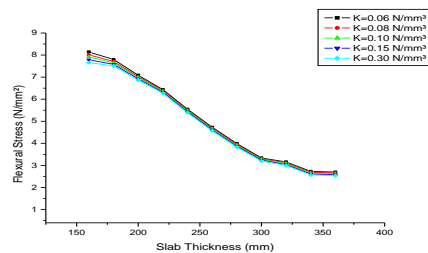


Fig. 5.9: Stresses in rigid pavement (single axle load = 220kN)

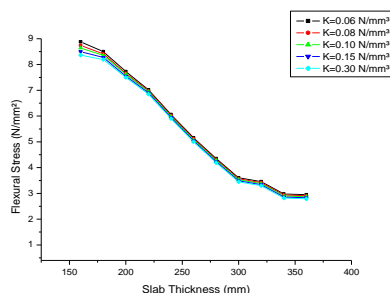


Fig. 5.10: Stresses in rigid pavement (single axle load = 240kN)

VI CONCLUSION

Based on the results of the research work, following conclusions were drawn:

- FEM techniques is more versatile in determining wheel load stresses.
- Design charts developed by using ANSYS software are slightly on a higher side when compared to values given by IRC 58 – 2002 design charts.[6]
- Westergaard’s equation under estimate edge wheel load stresses when compared with those obtained from FEM technique. The maximum deviation of the results of FEM analysis from that of Westergaard’s equation was 28.3%. [9]

VII REFERENCES

- [1] ANSYS Release 10.0 user’s, Manual, ANSYS, Inc. Canonsburg, PA, USA.
- [2] Chih Ping Wu and Pao – Anne Shen – “Dynamic Response of Concrete Pavements Subjected to Moving Load” Journal of Transportation Engineering / Sept/Oct. 1996, p-367.
- [3] Dr. K.Bhattacharya, “Edge Stress of Plain Concrete pavements” IE (I) Journal – CV.
- [4] Dr. S.K. Khanna, Dr. C.E.G.Justo, “High Engineering” 8th Edition 2001, published by New Chand & Bros, Civil Line Roorkee.
- [5] E.J.Yoder, M.W.Witczak, “Principal of Pavement Design”, 2nd Edition, A Wiley Interscience publication, New York.
- [6] IRC: 58 (2002) guidelines for the design of Rigid Pavements for Highways, Indian Roads Concretes, New Delhi.
- [7] Shuanfa Chen, Yi Jiang, & Bing Yang, “Finite Element Stress Analysis of Concrete Pavement with Subbase Voids” Department of Building Construction Management, Purdue University West Lafayette, IN47907, USA.
- [8] S.Santosh, T.Srinivas, K.Suresh & Prof. B.B.Panday, “Mechanistic Design of Concrete Pavement” Journal of IRC Oct/Dec 2006, Vol 67-3.
- [9] Westergaard, H.M. (1926), “Stresses in Concrete Pavements Computed by Theoretical Analysis”, Public Roads, Vol. 7, PP. 25 – 35.
- [10] Yoder EJ, “Principal of Pavement Design” Publisher John Wiley and Sons, Inc, US